American Mineralogist, Volume 70, pages 946–960, 1985

Raman spectra of gallium and germanium substituted silicate glasses: variations in intermediate range order

GRANT S. HENDERSON,[1] G. MICHAEL BANCROFT, MICHAEL E. FLEET

Departments of Geology and Chemistry
University of Western Ontario
London, Ontario, Canada N6A 5B7

AND DEREK J. ROGERS

Department of Chemistry
University of Waterloo
Waterloo, Ontario, Canada N2L 3G1

Abstract

Polarized Raman spectra of silicate and germanate glasses have been obtained in order to observe intermediate-range structural changes occurring within silicate melts upon the addition of network modifying cations.

The Raman spectra, when interpreted in terms of the vibrational bands observed for vitreous silica (v-SiO_2) show a number of significant systematic band shifts indicative of changes in intermediate range structure. v-SiO_2 exhibits a dominant vibrational band at 60–440 cm^{-1}. This band is attributed to symmetric stretching of bridging oxygens associated predominantly with rings of 6-membered SiO_4 tetrahedra. Bands at 490 cm^{-1} and 606 cm^{-1} are due to oxygen breathing modes associated with 4- and 3-membered rings respectively. With the addition of gallium and/or aluminum the small-membered ring vibrations become more dominant, indicating a gradual change in ring statistics and intermediate-range order. In particular, an increase in small-ring populations within the glass network is indicated. A shift in the 606 cm^{-1} band to lower frequencies upon the addition of Ga suggests preferential bonding of Ga/Al into the 3-membered rings as predicted by crystal chemical reasoning.

Addition of germanium to silicate glasses causes a shift of *all* vibrational bands to lower frequencies due to coupling of Ge with silicon. There is no preferential bonding of germanium into specific-sized rings of GeO_4 tetrahedra. The 490 cm^{-1} band of v-SiO_2 due to 4-membered rings does, however, shift to $\sim$440 cm^{-1} upon germanium addition.

Reduction in ring sizes and changes in ring populations may have a profound influence on petrologic phenomena. In particular, preferential bonding and changes in intermediate-range order can provide explanations for high pressure viscosity and density changes as well as the lack of observed nearest neighbor coordination changes.

Introduction

The importance of understanding the structure of melts relevant to igneous processes is evident from the intensive research being carried out in this field. Many of the dynamic and petrologically important processes occurring in igneous melts require knowledge of the melt structure. Most structural studies have been carried out on glasses with the assumption that the quenched melt, i.e., glass, provides a good approximation to the structure of the molten state; an approximation that appears valid (Mysen, 1983; Seifert et al., 1981; Okuno and Marumo, 1982; Domine and Piriou, 1983).

Raman spectroscopy in particular, has been shown to be a useful tool in the elucidation of glass structure. However, the interpretation of the data is dependent upon theoretical calculations of the vibrational properties of the system studied. Silicate glass systems have been interpreted in terms of the central force concept of Sen and Thorpe (1977), Galeener (1979), Thorpe and Galeener (1980); Bethe lattice theory (Laughlin and Joannopolous, 1977, 1978); Wilson FG-matrix and valence force fields (Bock and Su, 1970); large random networks (Bell and Dean, 1970, Bell et al., 1971; Dean, 1972); and standard coordinate and symmetry considerations of equivalent crystalline phases (Bates and Quist, 1972; Bates, 1972a, 1972b).

Mineral-composition glass studies have used calculations

[1] Present address: Department of Earth and atmospheric Sciences, York University, 4700 Keele St., Downsview, Ontario, M3J 1P3, Canada.

0003–004X/85/0910–0946$02.00

of vibrations in terms of SiO_4 or larger structural units found in silicate minerals (Brawer, 1975; Konijnendijk and Stevels, 1976a, 1976b; Furukawa and White, 1980; Mysen et al., 1980a, 1981, 1982a, 1982b; Siefert et al., 1981). A number of problems arise with these approaches since many of the vibrational bands are both band and molecular like and broadened due to variation in bond lengths and angles (Sen and Thorpe, 1977).

The present geological interpretation of melt structure is based upon the presence of anionic structural units within the melt and has been reviewed by Hess (1980) and Mysen (1983). Description of melts in terms of simple anionic units was suggested by Bockris et al. (1955) and Mackenzie (1960) for low-SiO_2 melts on binary metal oxide–silica joins. This idea has been extended by Hess (1971) to petrological melts, but tends to use thermodynamic and physical data to infer structure rather than direct structural studies, and extrapolates data obtained at low SiO_2 content to high-SiO_2 melts.

On the other hand, Mysen and co-workers have used direct structural studies and the ratio of non-bridging oxygens (NBO) to tetrahedral cations (T), NBO/T, to define various anionic units within the melt. The data of Mysen and co-workers, however, have been obtained primarily on the "high frequency" envelopes of their reported Raman spectra. According to model-dependent calculations by Bell et al. (1970), Stolen and Walrafen (1976), McMillan et al. (1982), Dowty (1982) and Dowty (1983), the vibrational bands in this high frequency region are highly localized. This means that one cannot infer structural units within the glasses other than SiO_4 tetrahedra with 1, 2 or 3 non-bridging oxygens. Interpretation of units such as dimers, chains and sheets from these high frequency bands is speculative (McMillan, 1984).

The approach we employ here is to investigate the "low frequency" envelope of glass Raman spectra. The vibrational bands in this region are coupled and no vibration will occur without exhibiting effects from the surrounding structure. The bands are therefore sensitive to the degree of polymerization (Matson et al., 1983) and most of the important intermediate range structural information may be contained in the weak features of this region (Evans et al., 1982).

Vitreous SiO_2 (v-SiO_2) and GeO_2 (v-GeO_2) are taken as representative spectra for an "almost" totally continuous random network. Their vibrational modes are then used to interpret the spectra of various mineral-composition glasses that are known to have three-dimensional network structures. This approach, which is admittedly speculative, does not rely on the use of specific structural units inferred from crystal structures. Additionally, since most mineralogically and petrologically important systems contain abundant SiO_2, their glass Raman spectra must include significant contributions from vibrations similar to those of v-SiO_2. Useful structural information, in particular intermediate range ordering, can therefore be obtained by using this approach.

Experimental

Glasses were obtained by melting stoichiometric mixtures of component oxides and carbonates in platinum crucibles at 1450°C for 1–2 hrs. The resulting melts were air quenched, checked for homogeneity by optical microscopy and electron microprobe, and if necessary, crushed and remelted. All glass compositions agreed to within ± 1 wt.% of nominal values by electron microprobe analysis.

Raman spectra were recorded with a Jarell–Ash 25-100 1.0 m Czerny–Turner double monochromator, a 129 digital cosecant stepping drive, an RCA 31034 selected photomultiplier and an SSR model 1105/1120 photon counting system. Spectra were excited by a Spectra Physics model 165-08 argon ion laser with the 488.0 nm laser line being used. A plasma filter was employed and laser power was 300–600 mW.

Polarized spectra of bubble free glass chips were obtained at 1 cm^{-1} intervals with a time constant of 2 to 5 seconds and a slit width of 2 cm^{-1}. A longer time constant would have produced a better signal to noise ratio for many of the glasses, however, further instrument time was unavailable. The signal to noise ratio is, however, significantly higher for glasses containing germanium, as germanate glasses are more efficient Raman scatterers (Seifert et al., 1981).

Experimental conditions were optimized using the 440 cm^{-1} or 490 cm^{-1} peak intensity of each composition, and spectra were calibrated against a neon arc lamp. Peak resolution is ± 10 cm^{-1} on the broad peaks and ± 5 cm^{-1} on the sharper peaks.

Replicate spectra from the same sample, different glass chips of the same sample, and duplicate glass syntheses were obtained. All bands and band shifts were reproducible. In addition, the $NaGaSi_3O_8$, $NaGaSi_2O_6$ and $NaGaSiO_4$ spectra were duplicated by S. K. Sharma, University of Hawaii, using longer run times and all of the band details of our spectra were shown to be completely reproducible.

Results

SiO_2

The polarized spectrum of vitreous SiO_2 (v-SiO_2) is shown in Figure 1 and band assignments are given in Table 1. The spectrum is similar to previously published results (cf. Wong and Angell, 1971, 1976).

The main features of the spectrum are the broad asymmetric polarized band between 60 and 440 cm^{-1}, the slightly polarized band at 800 cm^{-1}, the sharp bands at 490 cm^{-1} and 606 cm^{-1}, and the two broad high frequency depolarized bands at 1065 cm^{-1} and 1200 cm^{-1}. The band at 60–440 cm^{-1} is associated with symmetric stretching of the bridging oxygens (Bell and Dean, 1970; Hass, 1970; Bell et al., 1971; Sen and Thorpe, 1977; Laughlin and Joannopolous, 1977; Galeener, 1979). The 800 cm^{-1} band is a result of Si–O–Si bending (Bell and Dean, 1970; Hass, 1970; Galeener, 1979) and has been considered as two bands with longitudinal and transverse optical (LO/TO) splittings (Galeener and Lucovsky, 1976; Galeener et al., 1983a) at 800 cm^{-1} and 820 cm^{-1}. The 1065 cm^{-1} and 1200 cm^{-1} band have been assigned to antisymmetric stretching of the bridging Si–O–Si oxygens (Bell et al., 1971; Galeener, 1979) that have undergone LO/TO splitting due to long range Coulomb forces (Scott and

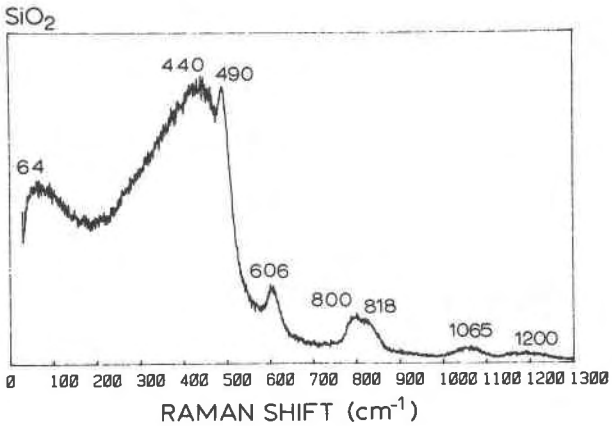

Fig. 1. Raman spectrum of vitreous SiO_2.

Porto, 1967; Galeener and Lucovsky, 1976; Galeener et al., 1983a).

Two features of the spectrum that have not been adequately explained by theoretical calculations, are the relatively sharp bands at 490 cm^{-1} and 606 cm^{-1}. These have been previously assigned by various workers to defects associated with broken Si–O bonds (Bates et al., 1974; Stolen and Walrafen, 1976; Lucovsky, 1979a, 1979b; Mikkelsen and Galeener, 1980).

The defect hypothesis has been questioned (cf. McMillan, 1984, p. 627) and most recent studies (e.g., Bell, 1982; Galeener, 1982a, 1982b, 1982c and Revesz and Walrafen, 1982) have assigned the 490 cm^{-1} and/or the 606 cm^{-1} bands to small-ring vibrations. The doubly bonded Si=O hypothesis of Phillips (1982) also appears questionable since it is apparently not consistent with molecular orbital calculations (cf. McMillan, 1984). One would also expect the vibrational mode of such a defect to occur at much higher frequencies than 490 cm^{-1} (Revesz and Walrafen, 1982).

Sharma et al. (1981) have concluded that the 490 cm^{-1} band is due to rocking of Si–O–Si bonds associated with coesite-like four-membered rings of SiO_4 tetrahedra within the glass network. Galeener (1982a, 1982b, 1982c) and Galeener and Geissberger (1983) have shown that the 606 cm^{-1} is a result of an oxygen-breathing mode associated with the formation of planar three-membered rings and the 490 cm^{-1} is assigned to planar or slightly puckered four-membered rings. Both small-membered ring concentrations are of the order of $\leq 1\%$.

We consider then, that v-SiO_2 consists of an almost continuous random network with an intermediate range structure of rings of SiO_4 tetrahedra. X-ray radial distribution function (RDF) studies have shown that while v-SiO_2 probably has rings of ≥ 3 SiO_4 tetrahedra; the network is overwhelmingly dominated by 6-membered rings (Konnert et al., 1982). These 6-membered rings are in turn both cristobalite and tridymite-like (Henderson et al., 1984). We would expect odd-membered rings to be fewer in number than even-membered rings. The former are more common in octahedral AB_3 random networks (Coey and Murphy, 1982).

The 60-440 cm^{-1} band therefore represents symmetric stretching of Si–O–Si bonds predominantly associated with 6-membered rings of SiO_4 tetrahedra with a minor contribution from 5-membered and >6-membered rings. The presence of the latter leads to the pronounced low-frequency tail of the 440 cm^{-1} band.

The assignment of the 490 cm^{-1} band to 4- rather than 3-membered rings is still debated. Bell (1982) and Revesz and Walrafen (1982) consider the 490 cm^{-1} band to be due to planar 3-membered rings and the 606 cm^{-1} band to unspecified symmetry or to rings attached to the rest of the network by lengthened Si–O bonds.

These explanations seem less likely since such lengthened Si–O bonds would tend to unnecessarily increase network strain and Si–O–Si bond energy. The pressure effects noted by Revesz and Walrafen (1982) on the 606 cm^{-1} band are equally applicable to a 3-membered ring model. In addition, the breathing modes of 4- and 3-membered rings in crystalline cyclosilicates occur around 500 cm^{-1} and 600 cm^{-1} respectively (cf. Griffith, 1969). The 4- and 3-membered ring assignment to the 490 cm^{-1} and 606 cm^{-1} bands does not involve introducing defects nor unusual bond configurations into the network. We therefore consider that, in general, the occurrence of these bands appears to indicate the presence of small-membered rings of SiO_4 tetrahedra.

GeO_2

The polarized spectrum of vitreous GeO_2 (v-GeO_2) is shown in Figure 2. Band assignments are given in Table 1. The Raman spectrum of v-GeO_2 has been described by Obukhov-Denisov et al. (1960); Bobovich and Tolub (1962); Morozov and Sharonova (1969); Stolen (1970); Galeener and Lucovsky (1976); Galeener (1979); Sharma et al.

Table 1. Band assignments (cm^{-1}) for SiO_2, GeO_2

v-SiO_2	v-GeO_2	Assignment
64, w, br, dp	45, w, br, dp	Acoustic
	342, m, p	Ge motion within the network
440, vs, br, p	420, vs, p	T-O-T symmetric-stretch, predominantly 6-membered rings
490, s, sh, p		Breathing, 4-membered rings
606, m, p	520, m, sh, p	Breathing, 3-membered rings
802 818 m, br, dp	500 650 m, br, dp	T-O-T bending
1065, w, br, dp 1200, vw, br, dp	855, w, br, dp 975, w, br, dp	T-O-T antisymmetric-stretch

vs = very strong
s = strong
m = medium
w = weak
vw = very weak
sh = shoulder
br = broad
p = polarized
dp = depolarized

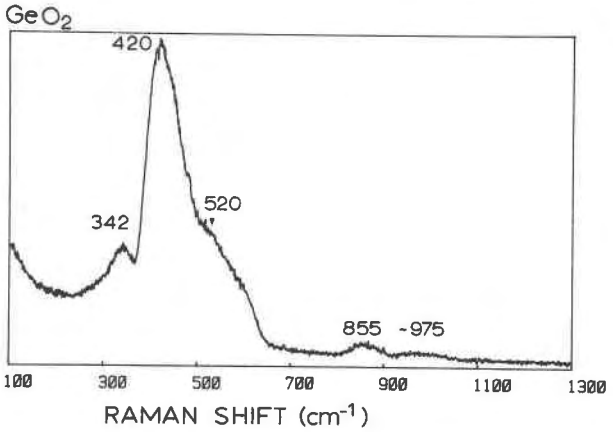

Fig. 2. Raman spectrum of vitreous GeO_2.

(1979b); Galeener (1980) and Seifert et al. (1981). Theoretical calculations have been carried out by Bell et al. (1968, 1970, 1971); Galeener and Lucovsky (1976) and Galeener (1979).

The band assignments for v-GeO_2 are similar to those of v-SiO_2 but are shifted to lower frequencies due to the heavier mass of germanium relative to silicon: i.e., Ge:Si = 72.59:28.086, (Bell et al., 1971). The 420 cm^{-1} band is assigned to symmetric-stretching (Hass, 1970; Bell et al., 1971; Verweij and Buster, 1979; Sharma et al., 1979b). This assignment is similar to that of the 440 cm^{-1} band described for v-SiO_2. The broad 500–600 cm^{-1} continuum is due to bending of the Ge–O–Ge while a "defect" mode is observed at 520 cm^{-1} (Verweij, 1979a, 1979b; Verweij and Buster, 1979; Galeener, 1979, 1980; Lucovsky, 1979a; Hass, 1970). This supposed "defect" mode at 520 cm^{-1} has been equated to the 606 cm^{-1} band in v-SiO_2 (Galeener, 1980; Galeener et al., 1983b; Seifert et al., 1981) and can therefore be attributed to the formation of smaller-membered GeO_4 rings.

The 855 cm^{-1} and 975 cm^{-1} bands are due to antisymmetric stretching of Ge–O–Ge with LO/TO splittings similar to the 1065 cm^{-1} and 1200 cm^{-1} band of v-SiO_2 (Hass, 1970; Galeener and Lucovsky, 1976; Verweij and Buster, 1979; Galeener et al., 1983a). The relatively sharp band at 342 cm^{-1} is primarily due to Ge motion within the network (Galeener et al., 1983b).

Gallium substitution into germanates of "albite" $Na(Ga_xAl_{1-x})Ge_3O_8$, "jadeite" $Na(Ga_xAl_{1-x})Ge_2O_6$, and "nepheline" $Na(Ga_xAl_{1-x})GeO_4$, compositions

The results and band assignments for compositions $x = 0.0$ to $x = 1.0$ are given in Table 2 and Figure 3. The major features of the spectra are in the 300 cm^{-1} to 700 cm^{-1} and 750 cm^{-1} to 1000 cm^{-1} ranges. For the $x = 0.0$ composition an intense band occurs at 442 cm^{-1} equivalent to the 420 cm^{-1} band of v-GeO_2, with a shoulder at 525 cm^{-1}. Upon addition of gallium the shoulder begins to shift to lower wavenumbers. This shoulder increases in intensity relative to the 442 cm^{-1} band on going from albite to nepheline-like compositions. The 442 cm^{-1} band shifts to higher wavenumbers; an effect noted by McMillan and Piriou (1982), reaching its maximum at $x = 0.5$ for albite and 0.75 for jadeite, then decreasing in frequency. The nepheline composition shows a continuous shift to higher wavenumbers. The high-frequency bands shift to lower wavenumbers, however the relative shift is greater for the lower of the two high-frequency bands. A band at 312 cm^{-1} for $x = 1.0$ occurs as a slight broadening of the 442 cm^{-1} peak and gradually becomes more distinct with increasing gallium content. It can be equated to the 342 cm^{-1} band of v-GeO_2. All bands are polarized to some extent, however, polarizability increases with Ga substitution.

Germanium substitution into gallosilicates of "albite" $NaGa(Ge_xSi_{1-x})_3O_8$, "jadeite" $NaGa(Ge_xSi_{1-x})_2O_6$ and "nepheline" $NaGa(Ge_xSi_{1-x})O_4$ composition

As expected the spectra of these compositions are predominantly SiO_2-like at high Si and GeO_2-like at low Si.

Table 2. Band positions (cm^{-1}) for the compositions $Na(Ga_xAl_{1-x})Ge_3O_8$, $Na(Ga_xAl_{1-x})Ge_2O_6$, and $Na(Ga_xAl_{1-x})GeO_4$

a) Band positions (cm^{-1}) for the composition $Na(Ga_xAl_{1-x})Ge_3O_8$.

x = 0.00	x = 0.25	x = 0.50	x = 0.75	x = 1.00
		≈333 sh(w)*	326 (w)*	312 (m)*
442 (vs)*	444 (vs)*	451 (bs)*	448 (vs)*	448 (vs)*
525 sh(s)*	525 sh(s)*	522 sh(s)*	513 sh(s)*	504 sh(s)*
839 (m)*	≈830 (m)*	823 (m)*	818 (m)*	789 (m)*
936 (m)*	≈930 (m)*	916 (m)*	906 (m)*	896 (m)*

b) Band positions (cm^{-1}) for the compositions $Na(Ga_xAl_{1-x})Ge_2O_6$.

x = 0.00	x = 0.25	x = 0.50	x = 0.75	x = 1.00
≈379 Sh(vw)*	-	319 (vw)*	317 (m)*	306 (m)*
454 (vs)*	456 (vs)*	465 (vs)*	462 (vs)*	452 (vs)*
525 sh(s)*	517 sh(s)*	513 sh(s)*	509 sh(s)*	506 sh(s)*
835 sh(m)*	825 sh(m)*	811 sh(m)*	800 (m)*	784 (m)*
926 (m)*	918 (m)*	910 (m)*	900 (m)*	879 (m)*

c) Band positions (cm^{-1}) for the compositions $Na(Ga_xAl_{1-x})GeO_4$.

x = 0.00	x = 0.25	x = 0.50	x = 0.75	x = 1.00
385 (w)*		308 (vw)*	300 (w)*	298 (m)*
464 (vs)*	463 (vs)*	469 (s)*	≈476 (s)*	475 sh(s)*
520 sh(s)*	511 sh(s)*	508 (s)*	506 (s)*	500 (vs)*
841 (m)*	824 sh(m)*	784 sh(w)*	785 sh(m)*	770 sh(m)*
917 (m)*	908 (s)*	885 (s)*	867 (m)*	866 (m)*

vs = very strong
s = strong
m = medium
w = weak
vw = very weak
sh = shoulder
* = polarizable

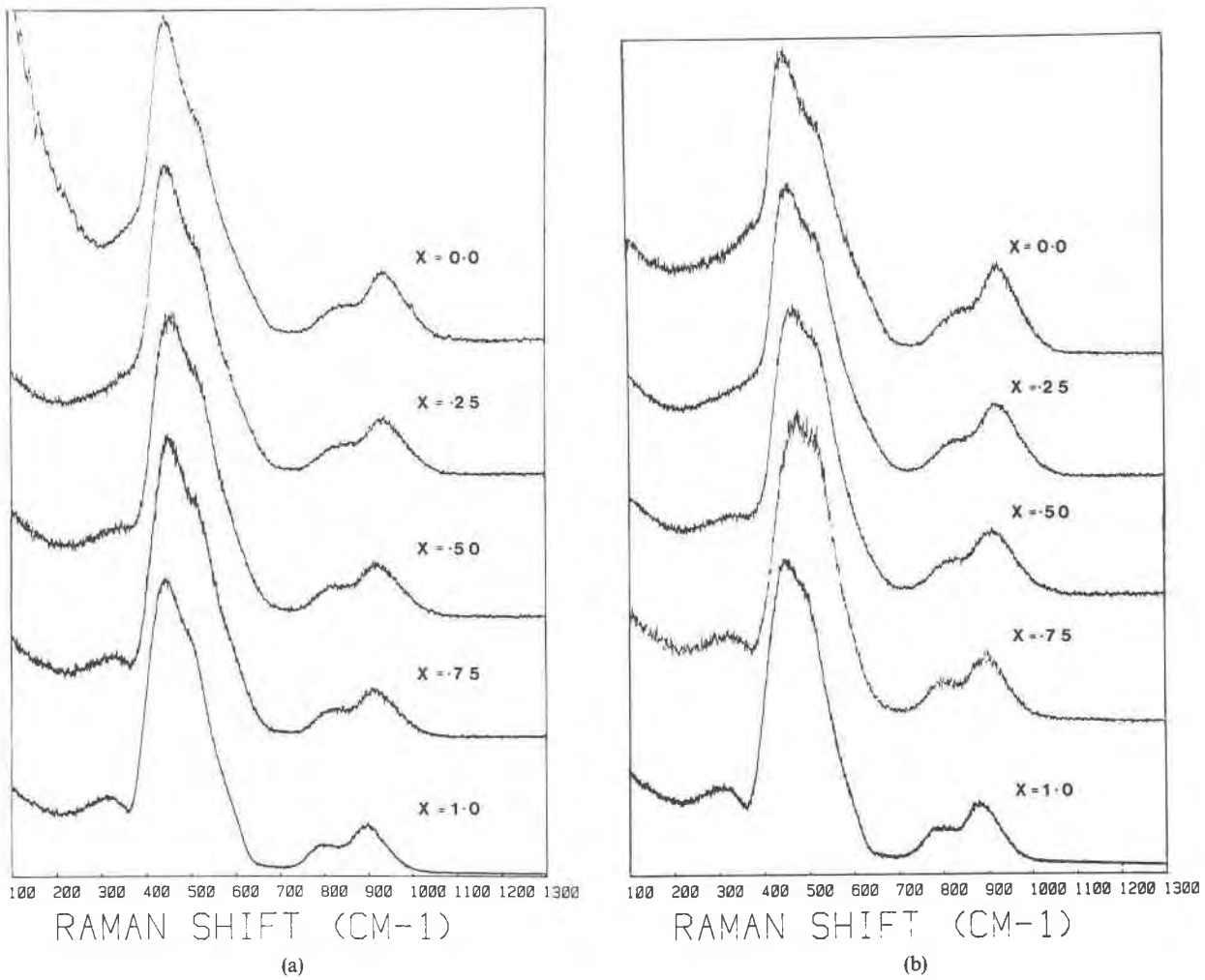

Fig. 3. Raman spectra for the compositions (a) $Na(Ga_xAl_{1-x})Ge_3O_8$; (b) $Na(Ga_xAl_{1-x})Ge_2O_6$; (c) $Na(Ga_xAl_{1-x})GeO_4$.

The results are shown in Table 3 and Figure 4. For $x = 0.0$ a strong asymmetric band occurs at 490 cm^{-1} with a shoulder at 562 cm^{-1} and possible shoulder at 357 cm^{-1}. We assign these 490 cm^{-1} and 562 cm^{-1} bands to Si–O–Si vibrations associated with the same structural units as those which cause, respectively, the 490 cm^{-1} and 606 cm^{-1} band observed in v-SiO_2. Similar 490 cm^{-1} and $\sim$600 cm^{-1} bands in Na-silicate glasses have been suggested to correspond to the 490 cm^{-1} and 606 cm^{-1} bands of v-SiO_2 (Hass, 1970). McMillan (1984) considers this unlikely but does suggest that they are due to similar vibrations.

It is known that band frequencies in this low-frequency region are highly sensitive to Si–O–Si angle and a systematic decrease in the frequencies of bands in this region may be related to increase in Si–O–Si angle with polymerization (McMillan, 1984). The feldspar compositions that we have used, while still essentially 3-dimensional networks, are slightly depolymerized by the addition of Na_2O. As such, one would expect a decrease in Si–O–Si angle and Galeener (1982a) has shown that with a decrease in Si–O–Si angle certain ring configurations become energetically more favorable.

The 490 cm^{-1} band is therefore assigned to symmetric-stretch of Si–O–Si bonds associated with 4-membered rings. This band is no longer purely a breathing mode as it has substantially broadened while the asymmetry is a result of Si–O–Si symmetric stretch associated with rings of more than 4 SiO_4 tetrahedra.

It is unlikely that the 490 cm^{-1} band is the equivalent of the 440 cm^{-1} band observed for v-SiO_2. For example, with the addition of K_2O along the K_2O–SiO_2 join, the 440 cm^{-1} band of V-SiO_2 is seen to decrease in intensity and disappear at 25 mole % K_2O while the 490 cm^{-1} band shifts to higher frequencies. A shift of 60 cm^{-1} is observed at the disilicate composition. Similar changes are observed for Na_2O–SiO_2 glasses (McMillan, 1984).

We would therefore expect for the Na(Ga, Al) silicate compositions used in this study, a decrease in intensity of

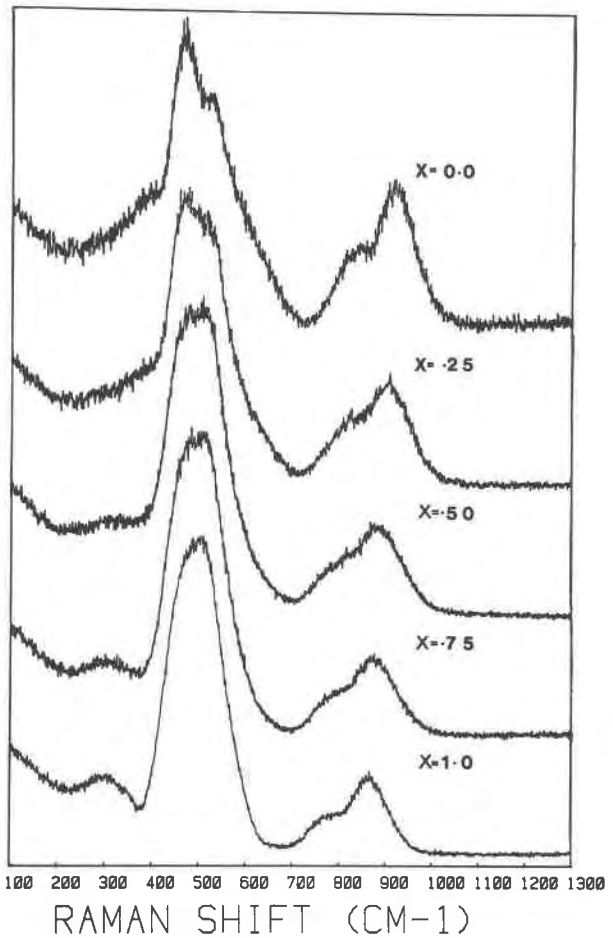

Fig. 3c.

the 440 cm^{-1} and a slight shift of the 490 cm^{-1} band to higher frequency. Any shift of the 440 cm^{-1} band to higher frequency is unlikely and a shift of 50 cm^{-1} does not seem at all reasonable.

Based on similar reasoning we assign the 562 cm^{-1} band to vibrations of Si–O–Si associated with 3-membered rings of TO_4 tetrahedra. The lower-frequency position of this band relative to the 606 cm^{-1} band of v-SiO_2 is a result of the addition of Ga to the composition. The heavier mass of Ga relative to Si shifts the bands involving Ga to lower frequencies. The shift of the 606 cm^{-1} band to 562 cm^{-1} would suggest that gallium is preferentially bonding into the 3-membered ring and its progressive shift to lower frequencies with increasing Ga content would tend to support this hypothesis.

High frequency Si–O–Si bending vibrations are observed at 794 cm^{-1} while broad asymmetric stretching occurs at 962 cm^{-1} and 1062 cm^{-1}. Addition of Ge shifts all bands to lower frequencies due to the higher mass of Ge relative to Si (Bell et al., 1970).

Gallium and germanium substitution into aluminosilicate glasses of "albite" $Na(Ga_xAl_{1-x})Si_3O_8$, $NaAl(Ge_xSi_{1-x})_3O_8$; "jadeite" $Na(Ga_xAl_{1-x})Si_2O_6$ and "nepheline" $Na(Ga_xAl_{1-x})SiO_4$ compositions

Unfortunately some of the high alumina compositions could not be glassed. The results for the glasses obtained are shown in Table 4 and Figure 5. As expected the results are similar to those of the Ge and Ga analogues. For the composition $NaAl(Ge_xSi_{1-x})_3O_8$ (Table 5, Fig. 6) band shifts relative to the Ga analogue are smaller due to the lighter atomic weight of Al with respect to Ga. Equivalent glasses of jadeite and nepheline compositions could not be glassed.

Discussion

Germanium substitution

In many previous Raman studies of silicate melts, an anionic structural model has been used to describe the melt

Table 3. Band positions (cm^{-1}) for the compositions $NaGa(Ge_xSi_{1-x})_3O_8$, $NaGa(Ge_xSi_{1-x})_2O_6$, and $NaGa(Ge_xSi_{1-x})O_4$

a) Band positions (cm^{-1}) for the compositions $NaGa(Ge_xSi_{1-x})_3O_8$.

x = 0.00	x = 0.25	x = 0.50	x = 0.75	x = 1.00
~357 sh(vw)*			317 sh(vw)*	312 (m)*
490 (vs)*	471 (vs)*	462 (vs)*	461 (vs)*	448 (vs)*
562 sh(s)*	559 sh(s)*	528 sh(s)*	527 sh(m)*	504 sh(s)*
794 (w)*	~654 (w)*	~665 (w)*	~674 sh(w)*	
		769 (vw)*		
962 (w)*	828 (w)*	858 (w)*	819 sh(w)*	789 (m)*
1062 (m)*	1038 (w)*	1047 (vw*	890 (m)*	896 (m)*

b) Band positions (cm^{-1}) for the compositions $NaGa(Ge_xSi_{1-x})_2O_6$.

x = 0.00	x = 0.25	x = 0.50	x = 0.75	x = 1.00
		328 sh(w)*	317 (m)*	306 (m)*
484 (vs)*	479 (vs)*	474 (vs)*	471 (vs)*	452 (vs)*
557 sh(s)*	~539 sh(m)*	~528 sh(m)*	~511 sh(s)*	506 sh(s)*
776 (w)*	~650 (w)*	~637 sh(w)*		
~960 sh(w)*	~831 (w)*	840 (w)*	~800 sh(vw)*	784 (m)*
1036 (m)*	997 (vw)*	1003 (vw)*	883 (w)*	879 (m)*

c) Band positions (cm^{-1}) for the compositions $NaGa(Ge_x(Si_{1-x})O_4$.

x = 0.00	x = 0.25	x = 0.50	x = 0.75	x = 1.00
384 sh(w)*		303 (w)*	286 (w)*	298 (m)*
481 sh(s)*	481 (vs)*	498 (vs)*	495 (vs)*	475 sh(s)*
528 (vs)*	510 (vs)*			500 (vs)*
~643 sh(vw)*	~643 sh(vw)*	~639 sh(vw)*	647 sh(vw)*	
748 (w)*	828 (w)*	~767 sh(vw)*	795 sh(w)*	770 sh(m)*
972 (w)*	948 (vw)*	850 (m)*	853 (m)*	866 (m)*

vs = very strong
s = strong
m = medium
w = weak
vw = very weak
sh = shoulder
* = polarizable

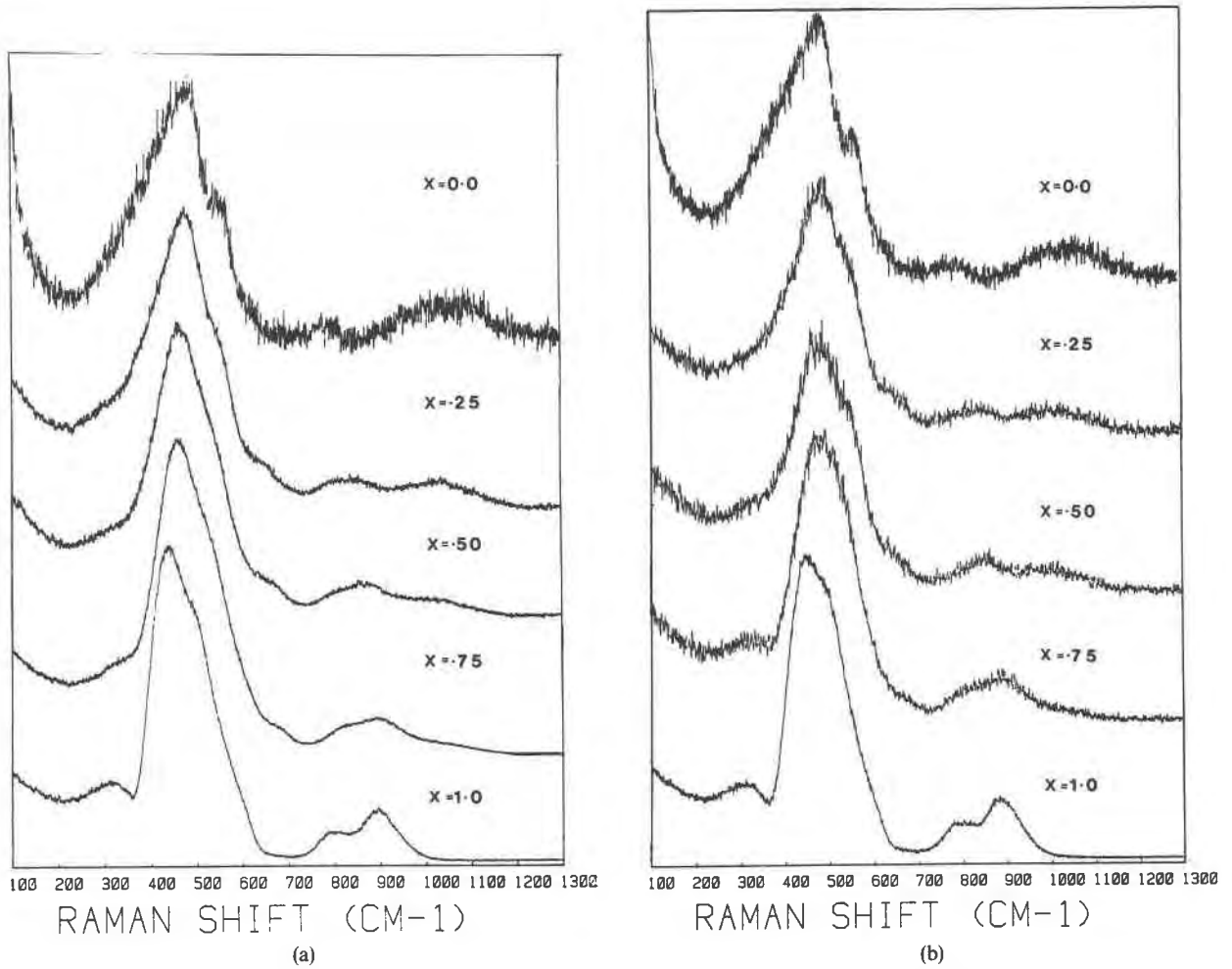

Fig. 4. Raman spectra for the compositions (a) $NaGa(Ge_xSi_{1-x})_3O_8$; (b) $NaGa(Ge_xSi_{1-x})_2O_6$; (c) $NaGa(Ge_xSi_{1-x})O_4$.

structure (Mysen et al., 1980a, 1981; Furukawa and White, 1980, Furukawa et al., 1981; Brawer and White, 1975, 1977). Unfortunately this approach infers the occurrence of structural units that may or may not occur in the melt but do occur in crystal structures. Such an approach is questionable. Mysen et al. (1981 p. 681) in fact state "... that this similarity (of crystalline and glassy $CaAl_2O_4$) is not proof of structural similarity ...".

Nearly all natural magmas have a NBO/T ratio of <1.0 (Mysen et al., 1981) and therefore by definition must consist predominantly of a three-dimensional network structure. This makes an investigation of three-dimensional network structure particularly interesting in terms of petrological processes (Seifert et al., 1982). Since v-SiO_2 is the classical network structure, interpretation of other network structures in terms of the bands observed in v-SiO_2 enables one to detect subtle structural differences between networks.

With the addition of Ge to the silicate compositions there is a continuous shift of all bands to lower frequencies indicating that the Ge has no preference for any particular network structure when replacing Si. Since the modes of this low-frequency region are coupled, with substitution of germanium into a specific intermediate-range structure one would expect to see a shift to lower frequency of only the corresponding Raman band resulting from that structure. However if germanium were substituting randomly for Si throughout the network we would observe a shift of all bands (both coupled low-frequency and localized high-frequency modes) to lower frequency. This is what is observed. This also implies that Ge glasses can be used as models for Si glasses and have the advantage of lower melting temperatures and being more efficient Raman scatterers (Seifert et al., 1981).

In addition, the main low-frequency Raman band undergoes a decrease in intensity on its low-frequency asymmetric side, as it shifts from 490 cm^{-1} to 442 cm^{-1} upon the addition of germanium. This indicates a narrowing of the T–O–T bond angle distribution and consequently a probable reduction in numbers of higher-membered rings

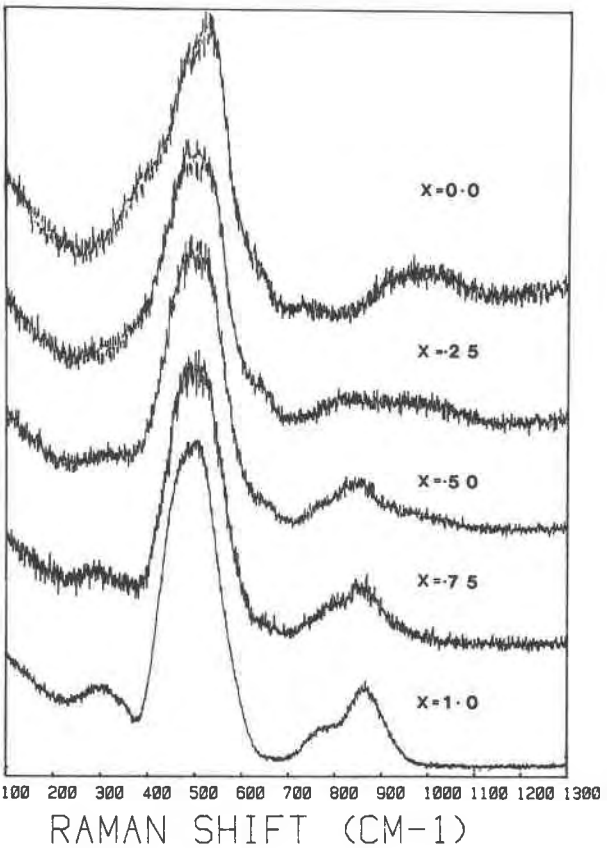

Fig. 4c.

of TO_4 tetrahedra. The shift of the 490 cm^{-1} band to 442 cm^{-1} suggests that these 2 bands result from similar vibrations associated with the same intermediate range structural unit. This may indicate that the germanate compositions have a predominant intermediate-range structure different to that of v-SiO_2.

The germanate spectra (Figs. 3 and 4) are strikingly similar to the v-GeO_2 spectrum (Fig. 2), and the present inferences on the structure of germanante glasses could be extended to the v-GeO_2 structure. We hesitate to do this because measured density data are fully consistent with a 6-membered ring structure for v-GeO_2. We recognize that the present band assignments are tentative and that further study of this problem is required. However, the decrease in intensity of the low-frequency tail to the 420 cm^{-1} band of the v-GeO_2 spectrum would seem to indicate a decrease in the number of higher-membered ring structures in v-GeO_2 compared to v-SiO_2.

Studies indicating that large discrepancies in the refractive index of germanosilicate glasses are related to germanate structure (Verweij et al., 1979) have indicated the occurrence of six [6] coodinated Ge. Verweij and Buster (1979), Kamiya and Sakka (1979), Sakka and Kamiya (1982) and Chakraborty and Condrate (1983) have inferred the presence of GeO_6 polyhedra on the basis of Raman, EXAFS, and RDF results.

Tetragonal GeO_2 with Ge in [6] coordination, has Raman frequencies of 170, 680, 700, 860 cm^{-1} (Scott, 1970). The coordination change from [4] to [6] has been inferred from shifts of v-GeO_2 bands to higher frequencies (Verweij and Buster, 1979). No such band shifts are observed in the present spectra and thus no germanium is considered to be in [6]-fold coordination. Similarly, the results of Kamiya and Sakka (1979), Sakka and Kamiya (1982) based on RDF and EXAFS studies are questionable. They carried out theoretical calculations of coordination numbers based on the "K approximation" technique (Leadbetter and Wright, 1972) for X-ray data. This technique is considered rather inaccurate for GeO_2 and generally indicates higher coordination numbers than expected (Leadbetter and Wright, 1972). The coordination numbers of 5.0 at around 20–30% Na_2O observed by Kamiya and Sakka (1979) could in fact be due to an increase in Ge–O bond length associated with an increase in numbers of smaller-membered rings.

Table 4. Band positions (cm^{-1}) for the compositions $Na(Ga_xAl_{1-x})Si_3O_8$, $Na(Ga_xAl_{1-x})Si_2O_6$, and $Na(Ga_xAl_{1-x})SiO_4$

a) Band positions (cm^{-1}) for the compositions $Na(Ga_xAl_{1-x})Si_3O_8$.

x = 0.00 (1)	x = 0.25 †	x = 0.50	x = 0.75 †	x = 1.00
453				357 sh(v)*
488		482 (vs)*		490 (vs)*
579		564 sh(s)*		562 sh(s)*
790		795 (w)*		794 (w)*
~1014				962 (w)*
~1123		~1066 (m)*		1062 (m)*

b) Band positions (cm^{-1}) for the compositions $Na(Ga_xAl_{1-x})Si_2O_6$.

x = 0.00	x = 0.25 †	x = 0.50	x = 0.75	x = 1.00
~450 (1)		~372 sh(vw)*		
485 (1)		484 (vs)*	486 (vs)*	484 (vs)*
570 (1)		561 sh(s)*	557 sh(s)*	557 sh(s)*
715 (1)				
780 (1)		773 (w)*	~775 (vw)*	776 (w)*
959 (2)		~1018 (w)*	1043 (m)*	~960 sh(w)*
1063 (2)			1091 (w)*	1036 (m)*

c) Band positions (cm^{-1}) for the compositions $Na(Ga_xAl_{1-x})SiO_4$.

x = 0.00	x = 0.25 †	x = 0.50	x = 0.75	x = 1.00
~436 (1)		389 sh(m)*	~391 sh(m)*	~384 sh(w)*
486 (1)		491 (vs)*	495 (vs)*	481 sh(s)*
565 (1)		550 (vs)*	545 (vs)*	528 (vs)*
705 (1)				
706 (1)		736 (vw)*	727 (vw)*	~643 sh(vw)*
945 (2)				
1014 (2)		~1005 (m)*	1004 (m)*	972 (w)*

vs = very strong
s = strong
m = medium
w = weak
vw = very weak
sh = shoulder

* = polarizable
† = unable to obtain spectrum
(1) = Taken from Siefert et al. (1982)
(2) = Taken from Mysen et al. (1981)

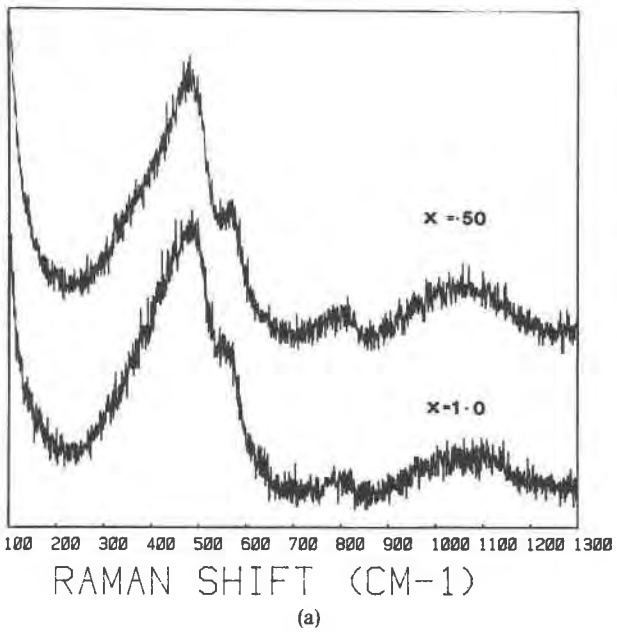

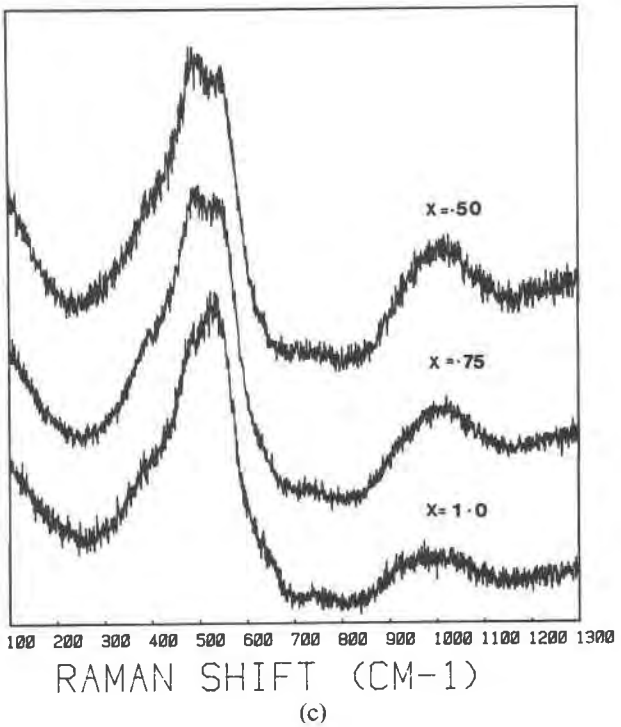

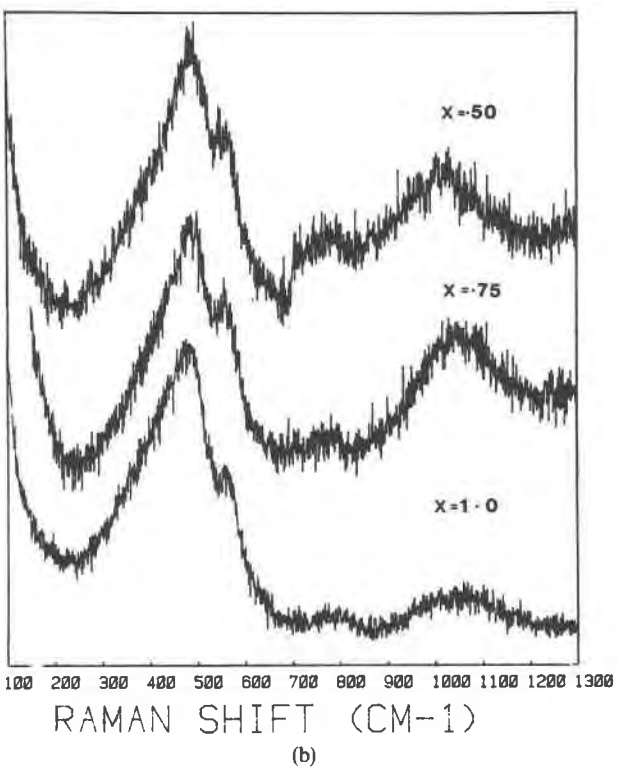

Fig. 5. Raman spectra for the compositions (a) $Na(Ga_xAl_{1-x})Si_3O_8$; (b) $Na(Ga_xAl_{1-x})Si_2O_6$; (c) $Na(Ga_xAl_{1-x})SiO_4$.

Gallium substitution

The results indicate that there is extensive coupling of Ga with Si/Ge. Additionally, the systematic shifts in the shoulder at $\sim$460 cm^{-1} to lower wavenumbers indicate preferential bonding of Ga/Al into the smaller structures associated with this vibrational mode. Mysen et al. (1980a), Virgo et al. (1980), Gaskell (1975), Vukcevitch (1972), De Jong et al. (1981) and Gaskell and Mistry (1975) have all suggested that the silicate or SiO_2 three-dimensional network is composed of at least two or more distinct structures. Mysen et al. (1980a, 1981) have also suggested that Al has a preference for the network structure while Seifert et al. (1982) showed that the proportion of rings with the largest T–O–T angle decreases with increasing Al/(Al + Si). This suggests aluminum has a preference for the network structure with the smallest T–O–T angle and largest T–O distance. The results reported here confirm that at least three distinct structures of intermediate-range order can be observed in the Raman spectra. In addition, on going from albite to nepheline composition, both gallium- and germanium-substituted glasses exhibit an increase in intensity of the band we assign to 3-membered rings. Across this compositional range there is an increase in network modifier content which should depolymerize the network. The increase in the small-membered ring vibrational band intensity may therefore indicate an increase in the proportion of smaller-membered rings in the order nepheline > jadeite > albite. The smaller rings make up about 50% of the total concentration of rings in the nepheline

Table 5. Band positions (cm^{-1}) for the compositions $NaAl(Ge_xSi_{1-x})_3O_8$

x = 0.00 (1)	x = 0.25	x = 0.50	x = 0.75	x = 1.00
453	463 (s)*	455 (s)*	451 (s)*	442 (vs)*
488	558 sh(s)*	556 sh(m)*	523 sh(m)*	525 sh(s)*
579	660 (w)*	666 (vw)*		
790	892 (vw)*	902 (m)*	842 sh(vw)*	839 (m)*
~1014	1025 (w)*		934 (m)*	936 (m)*
~1123	1116 (vw)*			

vs = very strong
s = strong
m = medium
w = weak
vw = very weak
* = polarizable
(1) Taken from Seifert et al. (1982)

compositions. No evidence of Ga/Al coordination changes from [4] to [6] fold coordination are observed.

The shift in the main band at 440 cm^{-1} to higher wavenumbers has been observed in silicate glasses by McMillan and Piriou (1982). They attributed the shift to an increase in the contribution of the 525 cm^{-1} shoulder and more recently to the formation of Si–O–Al bond pairs (McMillan et al., 1982). The band shift could be due in part to both effects. However, the band shift reverses at higher Ga concentrations for the albite and jadeite compositions. This should not occur if the shift were due solely to the above effects. At present no satisfactory explanation is available.

The high-frequency non-bridging oxygen bands (NBO) show a progressive decrease in wavenumber and increase in relative intensity as the compositions shift from albite to nepheline. The increase in intensity probably reflects an increase in numbers of NBO's associated with the increase in network modifier content of the glasses on going from albite to nepheline composition. However, this increase in NBO's could also be related to the formation of the planar 3-membered rings. These small rings are likely to be quite rigid (Thorpe, 1983) so that if significant quantities of the 3-membered rings are present within the network they could hinder 3-dimensional cross linking and therefore generate additional NBO's.

The decrease in frequency is due to coupling of Ga with the Si and Ge atoms in the smaller-membered rings. Both high-frequency bands shift to lower frequencies as each band represents a different normal mode associated with the same molecular structure (McMillan et al., 1982), which in this case would be the TO_4 tetrahedra with one or more NBO's.

Ring stability

A cursory survey of mineral structures reveals the existence of a wide variety of SiO_4 tetrahedral ring structures. For example, wadeite, benitoite, catapleiite, margarosanite, walastromite and high pressure $CaSiO_3$ all have 3-membered ring structures, eudialyte has 3- and 9-membered rings while the feldspars and SiO_2 structures are 4- and 6-membered, respectively. Germanium analogues of 6-, 4- and 3-membered ring structures are GeO_2 (6-membered), germanium feldspars (4-membered; Kroll et al., 1983) and the tetragermanates $K_2Ge_4O_9$ (Völlenkle and Wittmann, 1971), $K_2Ba[Ge_4O_9]_2$, $Na_2Ba[Ge_4O_9]_2$, $Rb_2Ba[Ge_4O_9]_2$, $Na_2Sr[Ge_4O_9]_2$ and $K_2Sr[Ge_4O_9]_2$ (Baumgartner and Völlenkle, 1978).

The stabilities of SiO_4 ring structures have been investigated by Gibbs and co-workers using molecular orbital calculations (cf. Gibbs (1981) for a summary of the present status of molecular orbital (M.O.) calculations as they apply to geological problems). Chakoumakos et al. (1981) have specifically studied the stability of 3-, 4-, 5- and 6-membered rings using siloxane molecules as models. They found that the experimental correlation of Si–O bond length increase with Si–O–Si angle decrease, is reproduced by theory. They also found that the 4- and 6-membered rings of various symmetries were quite stable and tended to achieve minimum energy Si–O–Si angles by assuming non-planar configurations, i.e., by puckering.

The 3-membered ring configuration was found by Chakoumakos et al. (1981) to be relatively unstable with a Si–O–Si angle of 130°. They did note, however, that its stability is increased by replacement of Si by Be or B atoms

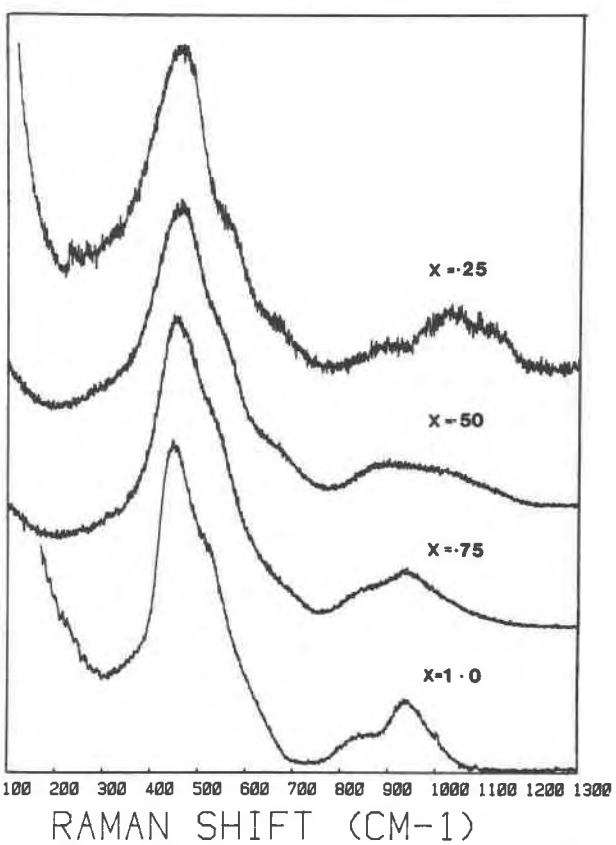

Fig. 6. Raman spectra for the composition $NaAl(Ge_xSi_{1-x})_3O_8$.

and by increasing pressure. On the other hand, Galeener (1982a) suggests that planar 3-membered rings are stable if one calculates the minimum energy Si–O–Si angle as ~152° (the value of v-SiO_2) rather than 142° as in the calculations of Chakoumakos et al. (1981). In addition to this, De Jong and Brown (1980) calculated the most stable Si–O–Al angle as 130°. This bond angle is the same as that calculated by Chakoumakos et al. (1981) for 3-membered rings.

Thus M.O. calculations indicate that a lengthening of the T–O bond occurs with decrease in T–O–T angle. The calculations also indicate that ring structures containing 4 or 6 TO_4 tetrahedra are stable ring configurations that tend to achieve minimum energy T–O–T angles by puckering. Planar 3-membered rings also appear to be stable configurations although less stable than 4- and 6-membered rings. Their stability would increase, however, with increasing pressure and, from simple crystal chemical reasoning, by substitution of Si^{4+} ($R = 0.26$Å) by Al^{3+} ($R = 0.39$Å), Fe^{3+} ($R = 0.49$Å) and Ga^{3+} ($R = 0.47$Å). Such a configuration is indicated in this study by the observation that it is the 3-membered ring that is preferentially bonded into by Ga/Al. It would also seem likely that the 3-membered rings will become more numerous within the melt with increasing pressure, (e.g., wadeite, Henshaw, 1955, a high pressure K, Zr silicate has a 3-membered ring structure), and for compositions with Al/Na > 1.0.

It appears that upon the addition of network modifiers that weaken the Si–O–Si bonds, the silicate network tries to maintain structural continuity during depolymerization by forming smaller-ring structures that gradually reduce in size as fragmentation of the overall network occurs. Cations such as Al^{3+}, Ga^{3+} and Fe^{3+}, which may act as both network modifiers and network formers, prefer to act as network formers by bonding into the smaller-ring structures. At high pressures this effect can contribute to the lack of observed high pressure coordination changes (Fleet et al., 1984).

Petrological applications

The concept of changes in intermediate range order and ring statistics can provide an explanation for high pressure effects previously attributed to coordination changes of Al^{3+} and Fe^{3+}. Past studies of petrological processes have related a number of effects to coordination changes (Waff, 1975, 1977) and variation in anionic units (Mysen et al., 1980a, 1980b, 1981; Seifert et al., 1982). Coordination changes have been used to explain such effects as: decrease in viscosity (Bottinga and Weill, 1972; Kushiro, 1976, 1978; Kushiro et al., 1976); CO_2 solubility (Mysen and Virgo, 1980a, 1980b); decrease in $Fe^{3+}/\Sigma Fe$ (Mysen and Virgo, 1978); Ni partitioning (Mysen and Kushiro, 1979; Mysen and Virgo, 1980c) and shift in liquidus field boundaries (Boettcher et al., 1982).

Unfortunately there is litte spectroscopic evidence for these proposed changes in coordination. De Jong et al. (1983) have recently carried out magic angle spinning ^{27}Al NMR and found no evidence for Al^{VI} in alumino silicate glasses. Sharma et al. (1979a) concluded that there is no coordination change of Al in jadeite glasses at high pressure and Fleet et al. (1984) have shown that there is neither a coordination change of Ga and Fe in sodium silicate glasses nor of Ge in GeO_2 glass at high pressure. Evidence for pressure-induced coordination changes has been based on inferred vibrational band shifts and increase in the intensity of NBO vibrations (Mysen et al., 1981). None of the spectral band changes observed by Sharma and Simmons (1981) upon change in coordination of Al from [4] to [6] in spodumene compositions have been observed along the various petrologically-important aluminosilicate joins.

We suggest that the increase in NBO vibration intensity could be related to the formation of small-membered rings while the increase in T–O bond length is a result of the decreased T–O–T angle associated with smaller ring formation. The concept of changes in ring statistics, ring size reduction, and preferential bonding of Ga/Al into the smaller rings can be followed as far as binary metal oxide/silica glasses for which three-dimensional network structures have been proposed (Tomlinson et al., 1958; Bockris and Kojonen, 1960; Robinson, 1969; Mysen et al., 1980a). If one accepts the lack of observed nearest-neighbor coordination changes to, say, 50 kbar as reality, and assumes that melt compression occurs preferentially through ring size reduction, then the viscosity, density and other petrological phenomena observed for silicate melts at pressure can be explained quite readily.

For example, the viscosities and densities of melts of jadeite ($NaAlSi_2O_6$) and albite ($NaAlSi_3O_8$) compositions undergo a number of changes with increasing pressure. Kushiro (1976) determined that the viscosity of $NaAlSi_2O_6$ melt decreased and density increased with pressure. These effects were interpreted as being due to a pressure-induced coordination change. Kushiro (1978) also found these effects in melts of $NaAlSi_3O_8$ compositions, although at a pressure 5 to 6 kbar greater than in jadeite melt. The proposed mechanism for the observed results was a coordination change of Al^{3+} from [4] to [6] causing depolymerization of the melt, weakening of (Si, Al)–O–(Si, Al) bonds and a decrease in viscosity.

As noted by Kushiro (1980), no evidence for 6-fold Al^{3+} has been found by Raman spectroscopy but he did suggest that shifts in Al K_α and K_β wavelengths by X-ray emission spectroscopy indicate 6-fold aluminum. Kushiro (1980) does note, however, that the K X-ray shifts could be explained by a change in the length of the T–O bond. This latter point is significant since lengthening of the T–O bond occurs with ring size reduction. We would argue that a more logical explanation of the viscosity and density changes for these melts is change in ring statistics while maintaining overall network continuity at the pressure observed. The viscosity decrease is due to the generation of smaller flow units within the melt (i.e., small-membered rings). Concomitant with the viscosity decrease is a density increase.

Studies of densified v-SiO_2 suggest that the increase in density can be related to a change to smaller average ring

size (McMillan et al., 1984; Revesz, 1972). McMillan et al. (1984) also suggest that the 3-membered rings are little affected by pressure as their T–O–T angle is already highly constrained. We would therefore suggest that change in ring statistics and formation of smaller-membered rings will increase the density of the melt. The albite viscosity and density changes are at higher pressures than jadeite melt as the albite melt initially has fewer smaller-membered rings.

A second example is the shift in liquidus field boundaries observed by Kushiro (1975), Boettcher et al. (1982) and Boettcher (1983). In these studies, olivine, pyroxene, silica minerals (Kushiro, 1975), diopside, albite (Boettcher et al., 1982) and SiO_2–H_2O–CO_2 (Boettcher, 1983) melt compositions are observed to undergo shifts in liquidus field boundaries. Again, these shifts are attributed to a coordination change of Al^{3+} from [4] to [6] and this change is based on the fact that a depolymerization reaction has occurred in which the density has increased and the viscosity decreased.

We must repeat that no structural data indicate any nearest-neighbor Al^{3+} coordination change and that the band shifts (in the above case, the X-ray emission spectroscopy data of Kushiro, 1980) used as evidence for such changes can be explained by an increase in T–O bond lengths associated with a decrease in T–O–T angle that occurs upon ring size reduction and change in ring statistics.

Conclusions

Our Raman spectra of silicate and germanate glasses can be interpreted in terms of the vibrational bands observed for v-SiO_2 and v-GeO_2. The concept of changes in ring statistics and progressive ring-size reduction with increasing network modifier content, suggest that the depolymerization reactions of previous workers probably result from a change in intermediate-range structure rather than the formation of discrete anionic species.

Addition of Ga indicates preferential bonding of Ga (and consequently of Al) into the 3-membered ring structure as predicted by crystal chemical and molecular orbital calculations. These 3-membered rings probably increase in stability with increasing pressure. Such ring-size reductions and preferential bonding can in turn be used to interpret a number of petrological phenomena previously attributed to nearest-neighbor coordination changes of Al^{3+}.

Germanium appears to substitute randomly for Si and shows no preference for a particular intermediate-range structure. A shift of the main Raman band in the Na-gallosilicate glasses to lower frequency upon the addition of germanium may indicate that Na-gallogermanates have a different intermediate range structure than v-SiO_2, with proportionately more smaller-membered TO_4 rings.

Acknowledgments

We thank D. E. Irish of the Chemistry Department, University of Waterloo, for use of Raman equipment. The manuscript was improved by comments from an anonymous referee and G. R. Rossman. This study was supported by Natural Sciences and Engineering Research Council of Canada operating grants to G. M. Bancroft and M. E. Fleet.

References

Bates, J. B. (1972a) Dynamics of β-quartz structures of vitreous SiO_2 and BeF_2. Journal of Chemical Physics, 56, 1910–1917.

Bates, J. B. (1972b) Raman spectra of α and β cristobalite. Journal of Chemical Physics, 57, 4042–4047.

Bates, J. B. and Quist, A. S. (1972) Polarized Raman spectra of β-Quartz. Journal of Chemical Physics, 56, 1528–1533.

Bates, J. B., Hendricks, R. W. and Snaffer, L. B. (1974) Neutron irradiation effects and structure of non-crystalline SiO_2. Journal of Chemical Physics, 61, 4163–4176.

Baumgartner, O. and Völlenkle, H. (1978) Die Kristallstruktur des Tetragermanats $K_2Ba[Ge_4O_9]_2$. Monatschefte für Chemie, 109, 1145–1153.

Bell, R. J. (1982) Phonon spectra of SiO_2: Comparison between computed and observed optical spectra. In Gaskell et al., Eds., The Structure of Non-Crystalline Materials, p. 417–425. Taylor and Francis, New York.

Bell, R. J. and Dean, P. (1970) Atomic vibrations in vitreous silica. Discussions of the Faraday Society, 50, 55–60.

Bell, R. J., Bird, N. F. and Dean, P. (1968) The vibrational spectra of vitreous silica, germania and beryllium fluoride. Journal de Physique C, 1, 299–303.

Bell, R. J., Dean, P. and Hibbens-Butler, D. C. (1970) Localisation of normal modes in vitreous silica, germania and beryllium fluoride. Journal de Physique C, 3, 2111–2118.

Bell, R. J., Dean, P. and Hibbens-Butler, D. C. (1971) Normal mode assignments in vitreous silica, germania and beryllium fluoride. Journal de Physique C, 4, 1214–1220.

Bobovich, Y. S. and Tolub, T. P. (1962) Raman spectra of alkali germanate glasses. Optics and Spectroscopy, USSR, 12, 269–271.

Bock, J. and Su, G. J. (1970) Interpretation of the infrared spectra of fused silica. Journal of the American Ceramic Society, 53, 69–73.

Bockris, J. O'M. and Kojonen, F. (1960). The compressibility of certain molten alkali silicates and borates. Journal of the American Ceramic Society, 82, 4493–4497.

Bockris, J. O'M., Mackenzie, J. D. and Kitchener, J. (1955) Viscous flow in silica and binary liquid silicates. Transactions of the Faraday Society, 51, 1734–1748.

Boettcher, A. L. (1983) CO_2 and H_2O in silicate liquids: SiO_2–H_2O–CO_2. Transactions of the American Geophyscial Union, 63, 339.

Boettcher, A. L., Burnham, C. W., Windon, K. E. and Bohlen, S. R. (1982) Liquids, glasses and the melting of silicates to high pressures. Journal of Geology, 90, 127–138.

Bottinga, Y. and Weill, D. F. (1972) The viscosity of magmatic liquids: A model for calculation. American Journal of Science, 272, 438–475.

Brawer, S. A. (1975) Theory of the vibrational spectra of some network and molecular glasses. Physical Review B, 11, 3173–3194.

Brawer, S. A. and White, W. B. (1975) Raman spectroscopic investigation of the structure of silicate glasses I. The binary alkali silicates. Journal of Chemical Physics, 63, 2421–2432.

Brawer, S. A. and White, W. B (1977) Raman spectroscopic investigation of the structure of silicate glasses II. Soda-alkali earth alumina ternary and quaternary glasses. Journal of Non-crystalline Solids, 23, 261–278.

Chakoumakos, B. C., Hill, R. J. and Gibbs, G. V. (1981) A molecu-

lar orbital study of rings in silicates and siloxanes. American Mineralogist, 66, 1237–1249.

Chakraborty, I. A. and Condrate, R. A. (1983) Raman spectra of potassium borogermanate glasses with high B_2O_3 contents. Journal of the American Ceramic Society, 66, C71–73.

Coey, J. M. D. and Murphy, P. J. K. (1982) An octahedral random network. Journal of Noncrystalline Solids, 50, 125–129.

Dean, P. (1972) The vibrational properties of disordered systems: numerical studies. Reviews in Modern Physics, 44, 127–168.

De Jong, B. H. W. S. and Brown, G. E. (1980) The polymerisation of silicate and aluminate tetrahedra in glasses, melts and aqueous solutions-I. Electronic structure of $H_6Si_2O_7$, $H_6AlSi_2O_7^-$ and $H_6Al_2O_7^{2-}$. Geochimica et Cosmochimica Acta, 44, 491–511.

De Jong, B. H. W. S., Keefer, K. D., Brown, G. E. and Taylor, C. M. (1981) Polymerisation of silicate and aluminate tetrahedra in glasses, melts and aqueous solutions-III. Local silicon environments and internal nucleation in silicate glasses. Geochimica et Cosmochimica Acta, 45, 1291–1308.

De Jong, B. H. W. S., Schramm, C. M. and Parziale, V. E. (1983) Polymerisation of silicate and aluminate tetrahedra in glasses, melts and aqueous solutions-IV. Aluminum coordination in glasses and aqueous solutions and comments on the aluminum avoidance principle. Geochimica et Cosmochimica Acta, 47, 1223–1236.

Domine, F. and Piriou, B. (1983) Study of sodium disilicate melt and glass by infrared reflectance spectroscopy. Journal of Noncrystalline Solids, 55, 125–130.

Dowty, E. (1982) Vibrations of tetrahedra in silicate glasses. (abstr.) Geological Society of America Abstracts with programs, 14, 477.

Dowty, E. (1983) Aluminum tetrahedra in silicate glasses: Normal coordinate vibrational analysis. Transactions of the American Geophysical Society, 64, 344.

Evans, K. M., Gaskell, P. H. and Nex, C. M. M. (1982) Modelling the medium range structure of SiO_2. In Gaskell et al., Eds., The Structure of Noncrystalline Materials, p. 426–438. Taylor and Francis, New York.

Fleet, M. E., Herzberg, C. T., Henderson, G. S., Crozier, E. D., Osborne, M. D. and Scarfe, C. M. (1984) Coordination of Fe, Ga and Ge in high pressure glasses by Mossbauer, Raman and X-ray absorption spectroscopy, and Geological implications. Geochimica et Cosmochimica Acta, 48, 1455–1466.

Furukawa, T. and White, W. B. (1980) Vibrational spectra and structure. Journal of Noncrystalline Solids, 38/39, 87–92.

Furukawa, T., Fox, K. E. and White, W. B. (1981) Raman spectroscopic investigation of the structure of silicate glasses-III. Raman intensities and structural units in sodium silicate glasses. Journal of Chemical Physics, 75, 3226–3237.

Galeener, F. L. (1979) Band limits and vibrational spectra of tetrahedral glasses. Physical Review B, 19, 4292–4297.

Galeener, F. L. (1980) The Raman spectra of defects in neutron bombarded and Ge rich GeO_2. Journal of Noncrystalline Solids, 40, 527–533.

Galeener, F. L. (1982a) Planar rings in vitreous silica. Journal of Noncrystalline Solids, 49, 53–62.

Galeener, F. L. (1982b) Vibrational evidence for intermediate range order in glasses. In Gaskell et al., Eds., The Structure of Noncrystalline Materials, p. 337–359. Taylor and Francis, New York.

Galeener, F. L. (1982c) Planar rings in glasses. Solid State Communications, 44, 1037–1040.

Galeener, F. L. and Lucovsky, G. (1976) Longitudinal optical vibrations in glasses: GeO_2 and SiO_2. Physical Review Letters, 37, 1474–1478.

Galeener, F. L. and Geissberger, A. S. (1983) Vibrational dynamics in silicon-30 substituted vitreous silicon dioxide. Physical Review B, 27, 6199–6204.

Galeener, F. L., Leadbetter, A. J. and Strongfellow, M. W. (1983a) Comparison of neutron, Raman and infrared vibrational spectra of vitreous SiO_2, GeO_2 and BeF_2. Physical Review B, 27, 1052–1078.

Galeener, F. L., Geissberger, A. S., Ogar Jr., G. W. and Loehman, R. E. (1983b) Vibrational dynamics in isotopically substituted vitreous germanium dioxide. Physical Review B, 28, 4768–4773.

Gaskell, P. H. (1975) Construction of a model for amorphous tetrahedral materials using ordered units. Philosophical Magazine, 32, 211–229.

Gaskell, P. H. and Mistry, A. B. (1975) High resolution electron microscopy of small amorphous particles. Philosophical Magazine, 32, 245–251.

Gibbs, G. V. (1981) Molecules as models for bonding in silicates. American Mineralogist, 67, 421–450.

Griffith, W. P. (1969) Raman studies on rock forming minerals. Part I. Orthosilicates and cyclosilicates. Journal of the Chemical Society (A), 1372–1377.

Hass, M. (1970) Raman spectra of vitreous silica, germania and sodium silicate glasses. Journal of Physics and Chemistry of Solids, 31, 415–422.

Henderson, G. S., Fleet, M. E. and Bancroft, G. M. (1984) An X-ray scattering study of vitreous $KFeSi_3O_8$ and $NaFeSi_3O_8$ and reinvestigation of vitreous SiO_2 using quasi-crystalline modelling. Journal of Noncrystalline Solids, 68, 333–349.

Henshaw, D. E. (1955) The structure of wadeite. Mineralogical Magazine, 30, 585–595.

Hess, P. C. (1971) Polymer model of silicate melts. Geochimica et Cosmochimica Acta, 35, 289–306.

Hess, P. C. (1980) Polymerisation model for silicate melts. In R. B. Hargraves, Ed., Physics of Magmatic Processes, p. 3–48. Princeton University Press, Princeton, New Jersey.

Kamiya, K., and Sakka, S. (1979) X-ray diffraction study of Na_2O–GeO_2 glasses and coordination numbers of germanium. Physics and Chemistry of Glasses, 21, 60–64.

Konijnendijk, W. L. and Stevels, J. M. (1976a) The structure of borosilicate glasses studied by Raman scattering. Journal of Noncrystalline Solids, 20, 193–224.

Konijnendijk, W. L. and Stevels, J. M. (1976b) Raman scattering measurements of silicate glasses and compounds. Journal of Noncrystalline Solids, 21, 447–453.

Konnert, J. H., D'Antonio, P. and Karle, J. (1982) Comparison of radial distribution function for silica glass with those for various bonding topologies: use of correlation function. Journal of Noncrystalline Solids, 53, 135–141.

Kroll, H., Strob, W., Nabbs, M. M., Pentinghaus, H., Baumbauer, H. U. and Grunwald, A. (1983) Order and anti-order in K and Na feldspars. 3rd Nato Advanced Study Institute on Feldspars, Feldspathoids and their paragenesis abstracts with programs, 8.

Kushiro, K. (1975) On the structure of silicate melt and its significance in magma genesis: Regularities in the shift of the liquidus boundaries involving olivine, pyroxene and silica minerals. American Journal of Science, 275, 411–431.

Kushiro, K. (1976) Change in viscosity and structure of melt of $NaAlSi_2O_6$ composition at high pressure. Journal of Geophysical Research, 81, 6347–6350.

Kushiro, K. (1978) Viscosity and structural changes of albite ($NaAlSi_3O_8$) melt at high pressure. Earth and Planetary Science Letters, 41, 87–90.

Kushiro, K. (1980) Viscosity, density and structure of silicate melts at high pressures and their geological applications. In R. B. Hargraves, Ed., Physics of Magmatic Processes, p. 93–120, Princeton University Press, Princeton, New Jersey.

Kushiro, K., Yoder, H. S. and Mysen, B. (1976) Viscosities of basalt, and andesite melts at high pressures. Journal of Geophysical Research, 81, 6351–6356.

Laughlin, R. B. and Joannopoulos, J. D. (1977) Phonons in amorphous silica. Physical Review B, 16, 2942–2952.

Laughlin, R. B. and Joannopoulos, J. D. (1978) The effect of second nearest neighbour forces on the vibrations of amorphous silica. Physical Review B, 17, 2790–2791.

Leadbetter, A. J. and Wright, A. C. (1972) Diffraction studies of glass structure III: Limitation of the fourier method for polyatomic glasses. Journal of Noncrystalline Solids, 7, 141–156.

Lucovsky, G. (1979a) Spectroscopic evidence for valence alternation pair defect states in vitreous SiO_2. Philosophical Magazine, B39, 513–530.

Lucovsky, G. (1979b) Defect controlled carrier transport in amorphous SiO_2. Philosophical Magazine, B39, 531–540.

Mackenzie, J. D. (1960) Modern Aspects of the Vitreous State. Butterworths, London.

Matson, D. W., Sharma, S. K. and Philpotts, J. A. (1983) The structure of high silica alkali silicate glasses. A Raman spectroscopic investigation. Journal of Noncrystalline Solids, 58, 323–352.

McMillan, P. (1984) Structural studies of silicate glasses and melts—applications and limitations of Raman spectroscopy. American Mineralogist, 69, 622–644.

McMillan, P. and Piriou, B. (1982) The structures and vibrational spectra of crystals and glasses in the silica alumina system. Journal of Noncrystalline Solids, 53, 279–298.

McMillan, P., Piriou, B. and Navrotsky, A. (1982) A Raman spectroscopic study of glasses along the joins silica-calcium aluminate, silica-sodium aluminate and silica-potassium aluminate. Geochimica et Cosmochimica Acta, 46, 2021–2038.

McMillan, P., Piriou, B. and Couty, R. (1984) A Raman study of pressure-densified vitreous silica. Journal of Chemical Physics, 81, 4234–4236.

Mikkelsen, J. C. and Galeener, F. L. (1980) Thermal equilibration of Raman active defects in vitreous silica. Journal of Noncrystalline Solids, 37, 71–84.

Morozov, V. N. and Sharonova, N. N. (1969) Vibrational spectra and structure of germanium-lead glasses. Optics and Spectroscopy, USSR, 26, 256–257.

Mysen, B. O. (1983) The structure of silicate melts. Annual Reviews in Earth and Planetary Sciences, 11, 75–97.

Mysen, B. O. and Kushiro, I. (1979) Pressure dependence of nickel partitioning between forsterite and aluminous melt. Earth and Planetary Science Letters, 42, 383–388.

Mysen, B. O. and Virgo, D. (1978) Influence of pressure, temperature and bulk composition on melt structures in the system $NaAlSi_2O_6$–$NaFe^{3+}Si_2O_6$. American Journal of Science, 278, 1307–1322.

Mysen, B. O. and Virgo, D. (1980a) Solubility mechanisms of CO_2 in silicate melts: a Raman spectroscopic study. American Mineralogist, 65, 885–899.

Mysen, B. O. and Virgo, D. (1980b) The solubility behavior of CO_2 melts on the join $NaAlSi_3O_8$–$CaAl_2Si_2O_8$–CO_2 at high pressures and temperature: a Raman spectroscopic study. American Mineralogist, 65, 1166–1175.

Mysen, B. O. and Virgo, D. (1980c) Trace element partitioning and melt structure: an experimental study at 1 atm pressure. Geochimica et Cosmochimica Acta, 44, 1917–1930.

Mysen, B. O., Virgo, D. and Scarfe, C. M. (1980a) Relations between anionic structure and viscosity of silicate melts: a Raman spectroscopic study. American Mineralogist, 65, 690–710.

Mysen, B. O., Seifert, F. and Virgo, D. (1980b) Structure and redox equilibria of iron bearing silicate melts. American Mineralogist, 65, 867–885.

Mysen, B. O., Virgo, D. and Kushiro, I. (1981) The structural role of aluminum in silicate melts: a Raman spectroscopic study at 1 atmosphere. American Mineralogist, 66, 678–701.

Mysen, B. O., Virgo, D. and Seifert, F. A. (1982a) The structure of silica melts: Implications for chemical and physical properties of natural magma. Reviews of Geophysics, 20, 353–383.

Mysen, B. O., Finger, L. W., Virgo, D. and Seifert, F. A. (1982b) Curve fitting of Raman spectra of silicate glasses. American Mineralogist, 67, 686–695.

Obukhov-Denisov, V. V., Sobelov, N. N. and Cheremisinov, V. P. (1960) Vibrational spectra of the modifications of germanium dioxide. Optics and Spectroscopy, USSR, 8, 267–270.

Okuno, M. and Marumo, F. (1982) The structures of anorthite and albite melts. Mineralogical Journal, 11, 180–196.

Phillips, J. C. (1982) Spectroscopic and morphological structure of tetrahedral oxide glasses. Solid State Physics, 37, 93–171.

Revesz, A. G. (1972) Pressure induced conformational changes in vitreous silica. Journal of Noncrystalline Solids, 7, 77–85.

Revesz, A. G. and Walrafen, G. G. (1982) Structural interpretation for some Raman lines from vitreous silica. In Gaskell et al., Eds. The Structure of Noncrystalline Materials, p. 360–368. Taylor and Francis, New York.

Robinson, H. A. (1969) Physical properties of alkali-silicate glasses: I, additive relations in alkali binary glasses. Journal of the American Ceramic Society, 52, 392–399.

Sakka, S. and Kamiya, K. (1982) Structure of alkali germanate glasses studied by spectroscopic techniques. Journal of Noncrystalline Solids, 49, 103–116.

Scott, J. F. (1970) Raman spectra of GeO_2. Physical Review B, 1, 3488–3493.

Scott, J. F. and Porto, S. P. S. (1967) Longitudinal and transverse optical lattice vibrations in quartz. Physical Review, 161, 903–910.

Sen, P. N. and Thorpe, M. F. (1977) Phonons in AX_2 glasses: From molecular to band like modes. Physical Review B, 15, 4030–4038.

Seifert, F. A., Mysen, B. O. and Virgo, D. (1981) Structural similarity of glasses and melts relevent to petrological processes. Geochimica et Cosmochimica Acta, 45, 1879–1884.

Seifert, F. A., Mysen, B. O. and Virgo, D. (1982) Three dimensional network structure of quenched melts in the system SiO_2–$NaAlO_2$, SiO_2–$CaAl_2O_4$ and SiO_2–$MgAl_2O_4$. American Mineralogist, 67, 696–717.

Sharma, S. K. and Simmons, B. (1981) Raman study of crystalline polymorphs and glasses of spodumene composition quenched from various pressures. American Mineralogist, 66, 118–126.

Sharma, S. K., Virgo, D. and Mysen, B. O. (1979a) Raman study of the coordination of aluminum in jadeite melts as a function of pressure. American Mineralogist, 64, 779–787.

Sharma, S. K., Virgo, D. and Mysen, B. O. (1979b) Relationship between density, viscosity and structure of GeO_2 melts at low

and high pressures. Journal of Noncrystalline Solids, 33, 235–248.

Sharma, S. K., Mammone, J. F. and Nicol, M. F. (1981) Raman investigation of ring configurations in vitreous silica. Nature, 292, 140–141.

Stolen, R. H. (1970) Raman scattering and infrared absorption from low lying modes in vitreous SiO_2, GeO_2 and B_2O_3. Physics and Chemistry of Glasses, 11, 83–87.

Stolen, R. H. and Walrafen, G. E. (1976) Water and its relation to broken bonds in defects in fused silica. Journal of Chemical Physics, 64, 2623–2631.

Thorpe, M. F. (1983) Continuous deformations in random networks. Journal of Noncrystalline Solids, 57, 355–370.

Thorpe, M. F. and Galeener, F. L. (1980) Central force model for the high frequency vibrational bands of glasses. Journal of Noncrystalline Solids, 35/36, 1197–1202.

Tomlinson, J. W., Hayes, M. S. R. and Bockris, J. O'M. (1958) The structure of liquid silicates part 2. Molar volume and expansivities. Transactions of the Faraday Society, 54, 1822–1834.

Verweij, H. (1979a) Raman study of the structure of alkaligermanate glasses I: Sodium and potassium metagermanosilicate glasses. Journal of Noncrystalline Solids, 33, 41–53.

Verweij, H. (1979b) Raman study of the structure of alkaligermanate glasses II: Lithium, sodium and potassium digermanosilicate glasses. Journal of Noncrystalline Solids, 33, 55–69.

Verweij, H. and Buster, J. H. J. M. (1979) The structure of lithium, sodium, potassium germanate glasses, studied by Raman scattering. Journal of Noncrystalline Solids, 34, 81–89.

Verweij, H., Buster, J. H. J. M. and Remmers, G. F. (1979) Refractive index and density of lithium, sodium and potassium germanosilicate glasses. Journal of Materials Science, 14, 931–940.

Virgo, D., Mysen, B. O. and Kushiro, I. (1980) Anionic constitution of 1-atmosphere silicate melts: Implications for the structure of igneous melts. Science, 208, 1371–1373.

Völlenkle, H. and Wittmann, A. (1971) Die Kristallstruktur des Kaliumtetragermanats. Monatschefte für Chemie, 102, 1245–1256.

Vukcevitch, M. R. (1972) A new interpretation of the anomolous properties of vitreous silica. Journal of Noncrystalline Solids, 11, 25–63.

Waff, H. S. (1975) Pressure induced coordination changes in magmatic liquids. Geophysical Research Letters, 2, 193–196.

Waff, H. S. (1977) The structural role of ferric iron in silicate melts. Canadian Mineralogist, 15, 198–199.

Wong, J. and Angell, C. A. (1971) Application of spectroscopy in the study of glassy solids Part II. Infrared, Raman, EPR and NMR spectral studies. Applied Spectroscopy Reviews, 4, 155–232.

Wong, J. and Angell, C. A. (1976) Glass Structure by Spectroscopy. Marcel Dekker, New York.

Manuscript received, August 10, 1984;
accepted for publication, April 25, 1985.